THE JOURNAL OF PHYSICAL CHEMISTRY C

Article

Cite This: J. Phys. Chem. C 2018, 122, 13884−13893

pubs.acs.org/JPCC

Additive Selection Strategy for High Performance Perovskite Photovoltaics

Guifang Han,[†] Harri Dharma Hadi,[‖] Annalisa Bruno,[†] Sneha Avinash Kulkarni,[†] Teck Ming Koh,[†] Lydia Helena Wong,[†,‖] Cesare Soci,[‡] Nripan Mathews,*[,†,‖] Sam Zhang,*[,§] and Subodh G. Mhaisalkar*[,†,‖]

[†]Energy Research Institute @NTU (ERI@N), Nanyang Technological University, Research Techno Plaza, X-Frontier Block, Level 5, 50 Nanyang Drive, 637553, Singapore

[‖]School of Materials Science and Engineering, Nanyang Technological University, Nanyang Avenue, 639798, Singapore

[‡]Division of Physics and Applied Physics, School of Physical and Mathematical Sciences, Nanyang Technological University, 21 Nanyang Link, 637371, Singapore

[§]Faculty of Materials and Energy, Southwest University, Chongqing 400715, China

Supporting Information

ABSTRACT: Although much of the initial progress in perovskite solar cells has been made by the archetypal $CH_3NH_3PbI_3$, incorporation of an additional cation such as formamidinium, cesium, and mixed halides have shown promising results in both stability and device performance. However, the role of the additional cations as well as the mixed halides is yet to be fully understood. In this work, we investigate the role of different additives including group I alkali metal cations (K, Rb, Cs and NH_4) and halide anions (Br and I) on double-cation perovskites, i.e., $[(MAPbBr_3)_{0.15}(FAPbI_3)_{0.85}]$. A notably longer charge carrier lifetime is achieved for perovskite films with additives and may be attributed to defect passivation. Selection rules are put forward based on the effect of the ionic size of an additive on phase stabilization and defect passivation. Addition of complementary size cation with respect to cation size of the parent perovskite, mainly helps stabilizing the perovskite phase by tuning tolerance factor, while addition of the similar size cation/anion, acts as defect passivator. The performance improvement of devices fabricated using NH_4I as additive well supports this hypothesis, and offers yet another pathway toward harnessing the multitude of perovskite compositions to achieve high performing solar cells and perhaps other optoelectronic devices.

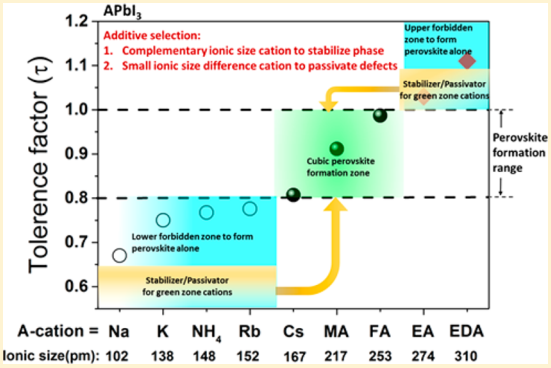

1. INTRODUCTION

Perovskites have cemented their position as the most efficient solution processed solar cells and their viability for industrialization is seriously being considered.[1−3] Formamidinium (FA) based perovskites have shown greater thermal stability than methylammonium (MA) perovskites, however,[4−7] FA-based perovskites resulted in a hexagonal yellow nonperovskite δ-phase at room temperature resulting in poor device performance. Subsequently, considerable efforts were made to achieve stable photoactive black α-$FAPbI_3$ perovskite phase through the use of the mixed-cation approach i.e. addition of a small amount of MA in $FAPbI_3$ perovskites.[8,9] The perovskite prepared using the mixed cation approach not only improves phase stability but also boosts the device performance.[10] Successively, efforts were made to improve the performance by means of mixed cation and halide based perovskites [e.g., $MA_{0.17}FA_{0.83}Pb(I_{0.83}Br_{0.17})_3$] for solar cells.[10−12] The mixed cation combination of Cs/FA[13,14] and Cs/MA/FA (triple cation) system has been reported to form a more pure and low defect density perovskite phase.[15−17] It has been noted that larger size difference between Cs (ionic radius of 167 pm), and FA (ionic radius 253 pm) could tune the effective tolerance factor (τ) of the final perovskite composition into suitable range ($0.8 < \tau < 1$).[13,15] X-ray photoelectron spectroscopy reveals that addition of Cs helps to push the composition of obtained film close to stoichiometric ratio and downshifts the valence band position.[17] Subsequently, the addition of Rubidium (ionic radius 152 pm) iodide (RbI) into a triple-cation perovskite system to form a quadruple-cation (RbCsMAFA) has been demonstrated to improve the device performance.[18] It has been discovered that the addition of RbI not only improves the crystallinity but also suppresses defect migration in perovskite.[19] The low trap-assisted charge-carrier recombination and low series resistance might be the possible reasons for the improvement of device performance with

Special Issue: Prashant V. Kamat Festschrift

Received: January 29, 2018
Revised: March 24, 2018
Published: March 25, 2018

DOI: 10.1021/acs.jpcc.8b00980
J. Phys. Chem. C 2018, 122, 13884−13893

incorporation of RbI.[20] KI and NH_4I as additives in different perovskite systems have also been reported.[21−23] During the revision of our work, alkali metal doping in perovskite solar cells has been reported by both Son et al.[24] and Tang et al.[25] They have demonstrated that KI addition improves the efficiency of perovskite solar cell, and at the same time dramatically reduces or totally overcomes the hysteresis behaviors. Theoretical investigations have suggested that vacancies (V_{MA}, V_{Pb} and V_I) and interstitials (MA_i, Pb_i and I_i) are the most likely defects in $MAPbI_3$ due to their lower formation energies.[3,26,27] In our previous work, it has been demonstrated that surface recombination was the dominant process in single crystal perovskite as well as polycrystalline perovskite solar cells, and both cations and halogen are deficient on the surface of perovskite films.[28,29] The surface treatment with MABr solution effectively compensates MA cation and Br/I anion deficiencies and thus reduces the trap density and dramatically improves the solar cell performance.[30] Although the additives effectively improve the solar cell performance of perovskite system, the role of the additives (cation and anion) is not yet very clear.

In this work, we have studied the effect of both cation (Cs, Rb, NH_4, and K) and anion (I and Br) as additives on optical, structural and electronic properties of the resultant perovskite film. The cations were chosen from the family of group I elements, i.e., alkali metals. Ammonium (NH_4) cation was selected due to its ionic size resemblance to Rb, i.e., 148 pm vs 152 pm. The iodide and/or bromide salts of Cs, Rb, K, and NH_4 were used as additives in small mole percentages (1%, 5%, and 10%) in the double cation perovskite precursor $(MAPbBr_3)_{0.15}(FAPbI_3)_{0.85}$ (as matrix, marked as "D"). We have also fabricated the prototype devices with NH_4I as an additive at various mole percentages (0%, 5% and 10%) to understand the effect of additive on the device performance and also to validate the results obtained from optical and photophysical characterization. We believe that this work will open up the novel possibilities of the composition design for perovskite to enhance the solar cell and other optoelectronic device performance.

2. EXPERIMENTAL METHODS

2.1. Film and Device Fabrication. Fluorine doped tin oxide (FTO, TEC 15, Nippon Sheet Glass Co., Ltd., Japan) substrates were etched using Zn powder and 2 M hydrochloric acid. The etched FTO substrates and glass slides were subsequently cleaned with Decon soap solution, deionized water and finally with ethanol. A thin compact layer of TiO_2 was deposited using a solution of titanium diisopropoxide bis(acetylacetonate) (75 wt % in isopropanol) and absolute ethanol (ratio 1:9 by volume) by spray-pyrolysis at 450 °C on FTO substrates. A mesoporous TiO_2 film was deposited by spin-coating TiO_2 paste (30 NR-D, Dyesol) diluted with ethanol (1:5.5 w/w) on the substrate and calcined at 500 °C for 30 min. Then 0.1 M bis-(trifluoromethane)sulfonimide lithium salt (Li-TFSI) in acetonitrile was spin coated to dope mesoporous TiO_2 according to the report by Giordano et al.[31] The doped substrates were annealed at 450 °C for 30 min and then transferred into an N_2 filled glovebox immediately after cooling to 150 °C.

FAI and MABr were purchased from Dyesol. PbI_2 and $PbBr_2$ are from TCI, and all the other chemicals are from Sigma-Aldrich. A mixed solution of FAI (1M), PbI_2 (1.1 M), MABr (0.2 M), and $PbBr_2$ (0.2 M) were dissolved in dimethylformamide:-dimethyl sulfoxide 4:1(v:v). The 1.5 M CsI, RbI, KI, and NH_4I stored solution in DMSO were added into the mixed solution forming the composition required. Because of the limited solubility of RbBr and KBr in DMSO, they were directly mixed in the powder form in the perovskite precursor solution of double cation. The perovskite layer was deposited by single step method as reported in literature.[15] In brief, the perovskite solution was spin-coated on the substrate at two different spin coating speeds, i.e., at 1000 rpm for 10 s and 6000 rpm for 30 s, respectively. During the second spinning step, 100 μL of chlorobenzene was dropped on the spinning substrate after 15 s. The substrates were subsequently annealed at 100 °C for 60 min. For film characterization, perovskites films were prepared on the glass substrate.

70 mg Spiro-OMeTAD was dissolved in 1 mL chlorobenzene with 28 μL of *tert*-butylpyridine, 16.9 μL of lithium bis-(trifluoromethylsulfonyl) imide (with a concentration of 520 mg/mL in acetonitrile), and 14 μL of cobalt dopant (with a concentration of 18 mg in 50 μL acetonitrile) added in. The spiro moiety was spin coated on the top of the perovskite films at 4000 rpm, 30 s. The gold counter electrode was deposited using the thermal evaporation method.

2.2. Characterization. The crystallographic information on the perovskite films were analyzed by Bruker AXS (D8 ADVANCE) X-ray diffractometer with Cu Kα radiation and a step of 0.02°. Absorption spectra of perovskite films were collected by UV−vis with a Shimadzu UV3600 spectrophotometer. The topographical images were recorded by using field emission scanning electron microscopy (FESEM, JEOL, JSM 7600F).

Carrier lifetime of perovskite films with different additives on glass substrates were measured using time-resolved photoluminescence (TRPL) analysis. The system consists of a microscope based PL setup with an excitation and emission collection path from the same side. The measurements were realized using a VIS-NIR microscope objective (10×, NA = 0.65). Light excitation was provided by laser diodes at 405 nm (Pico Quant LDH Series P−C-405B) with 60 ps pulse duration and 40 MHz repetition rate. The beam spot size was about 2 μm. The signal from the Single Photon Avalanche Diode (Laser 2000, Model $PD-50-CTE) detector was acquired by a time-correlated single photon counting card.

For the photovoltaic measurements, all devices with 5 × 5 mm^2 active area were measured by using solar simulator (San-EI Electric, XEC-301S) under AM 1.5G standard condition with a 3 × 3 mm^2 metal mask to precisely confine the area. The efficiency was obtained from a reverse scan at a scan rate of 0.1 V/s. Current−voltage ($J-V$) characteristics were recorded using a Keithley (model 2612A) digital source meter.

3. RESULTS AND DISCUSSION

In the selection of the additives, care has to be taken such that the additives should not introduce any nonperovskite phase, the band gap as well as the chemical properties of the matrix should not be altered. For that purpose, Goldschmidt tolerance factor (τ) provides a good guidance. It is an empirical index, widely used to predict the possibility of ABX_3 perovskite structure formation: τ in the range of $0.8 < \tau < 1.0$ favors ideal cubic structures or a distorted perovskite structure with tilted octahedra.[18,32] $\tau > 1.0$ or $\tau < 0.8$ indicates negligible possibility of perovskite phase formation.[33,34] τ is calculated using $\tau = (R_A + R_X)/[\sqrt{2}(R_B + R_X)]$, where R_A, R_X, and R_B are the diameter of component A, X, and B respectively.[33] For $APbI_3$ perovskite structure, the τ-values for perovskites with different "A"-site cations were calculated to predict the formation of stable perovskite phase. The different

DOI: 10.1021/acs.jpcc.8b00980
J. Phys. Chem. C 2018, 122, 13884−13893

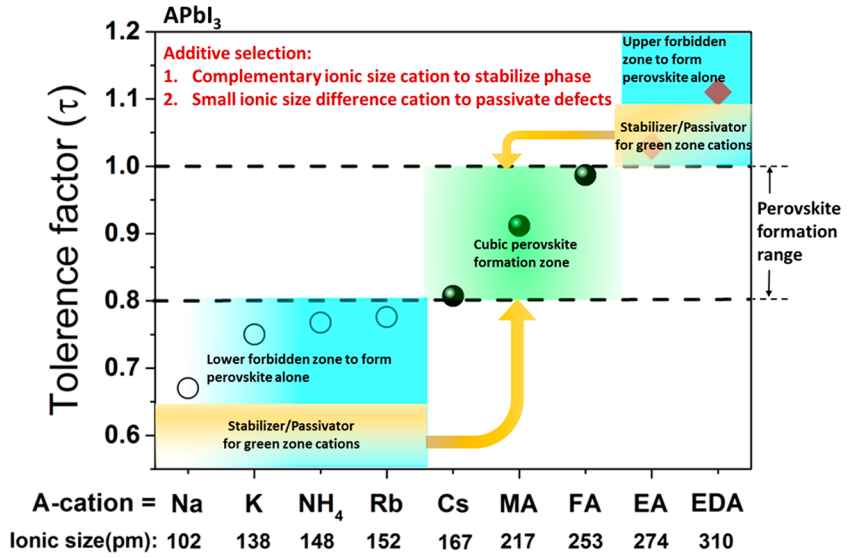

Figure 1. Calculated tolerance factors (τ) for different cations (A) in $APbI_3$ perovskite system. It turns out that the commonly used cations namely Cs, MA, and FA give rise to a τ-value in the range of 0.8−1.0, indicating the tolerance requirements for the formation of the cubic perovskite phase structure (green color in the figure). These cations can serve as additives to one another in unlimited amount without compromise in phase structure. Ethylammonium (EA) and ethylenediamine (EDA) cations are too big, giving rise to a tolerance factor of more than 1.0 thus fell into the "upper forbidden zone" and cannot form perovskite alone. The group I alkali metal cations (Na, K, Rb) and NH_4 have a τ-value less than 0.8 and thus fell into the "lower forbidden zone", not forming perovskite themselves. However, all cations of lower or upper "forbidden zone" can be used as additives into those cations in "cubic perovskite formation zone" for phase stabilization and defect passivation. To stabilize the perovskite phase (stabilizer), a larger ionic size difference between additive and parent perovskite cations is preferred, while to passivate the defects (passivator) in the perovskite matrix, a small ionic size difference benefits.

"A"-site cations used for calculation were alkali metals Na, K, Rb (group I elements), and commonly used Cs and MA, FA, NH_4, and larger size ethylammonium (EA) and ethylenediammonium (EDA). The results obtained from τ calculation were tabulated in Table S1 and plotted in Figure 1. The obtained values of τ fall into three categories: the commonly used Cs, MA and FA, which can easily form a perovskite phase, are in the range of $0.8 < \tau < 1.0$ (termed "cubic perovskite formation zone"), appearing in the middle of the space of tolerance factor vs composition (ionic size); On the other hand, Na, K, NH_4, and Rb these nonperovskite cations having $\tau < 0.8$ (termed "lower forbidden zone) appears at the lower left corner in this space; and the upper right corner sees EA and EDA with tolerance factor greater than 1.0 (termed "upper forbidden zone") also not able to form perovskite structure alone (c.f. Figure 1). Here, "forbidden zone" implies that the τ-values of cations falling in this zone are not able to form a perovskite phase alone but can be used as an additive in optimum amount of addition. As Cs, MA, and FA cations have ability to form the pure perovskite phase alone, within these elements, it can be served as an additive with indefinite amount without causing collapse of the perovskite structure. As Na, K, NH_4, Rb, EA, and EDA cations could not form an $APbI_3$ type "pure" perovskite phase themselves, they can be added with an optimum amount in perovskite matrix to avoid nonperovskite phase formation.

Even in the "cubic perovskite formation zone", both boundaries should be avoided for structural stability: as $FAPbI_3$ has a high τ ($\approx$ 1.0) at the upper boundary of the "cubic perovskite formation zone", nonphotoactive δ-$FAPbI_3$ yellow phase is prone to form during the fabrication process.[35] Addition of an additive to stabilize the perovskite matrix means bringing down the τ-value less than 1.0. Addition of a small amount of Cs (for instance 10%) from the lower "forbidden zone" to the upper boundary $FAPbI_3$ effectively avoids formation of the δ-phase (stabilizes the structure).[14] As $MAPbI_3$ has tolerance factor not too much lower than $FAPbI_3$, it needs much more MA addition (for instance 20%) to stabilize $FAPbI_3$.[8,9] At the lower boundary, it is difficult for $CsPbI_3$ ($\tau \approx 0.8$) to form the photoactive black phase at room temperature. Addition of an additive should be chosen to adjust the τ-value more than 0.8. Zhang et al.[36] have demonstrated the same concept with an addition of 2.5% of EDA (τ = 1.1) into $CsPbI_3$ matrix (τ = 0.8) stabilizes the perovskite matrix obviously owing to the fact that the overall τ value (0.81) is now away from the boundary. Therefore, to stabilize the perovskite phase, additive cation with larger ionic size difference with that of matrix cation is better choice.

$MAPbI_3$ has a τ-value of ~0.9, right in the middle of the "cubic perovskite formation zone", thus it is easy for $MAPbI_3$ to form the stable black phase. Recently it has been reported[37] that up to 25% EA cation has been successfully incorporated into $MAPbI_3$ without formation of the secondary phase. The authors attributed this result to the smaller molecular globularity resulting from the asymmetric of molecule, but a simply mixture rule calculation of the resultant τ still falls at about the middle of the "cubic perovskite formation zone" (0.96). However, further detailed crystal structure analysis should be carried out to clarify the real connection of all atoms inside this compound, which is still a big challenge for organic−inorganic hybrid perovskites.

As such, the selection rule of cation is such that the τ of the resultant system should be in the "cubic perovskite formation zone" ($0.8 < \tau < 1.0$) and away from boundary. An optimum amount of cations addition from both lower or upper "forbidden zone" brings the structural stability to the perovskite matrix by maintaining τ value toward the middle of the cubic perovskite formation zone, perhaps a controlled amount of addition to obtain a τ value around 0.9 may be ideal to make the system even more stable as long as no formation of a secondary phase. However, when additives are added in, especially, from the

DOI: 10.1021/acs.jpcc.8b00980
J. Phys. Chem. C 2018, 122, 13884−13893

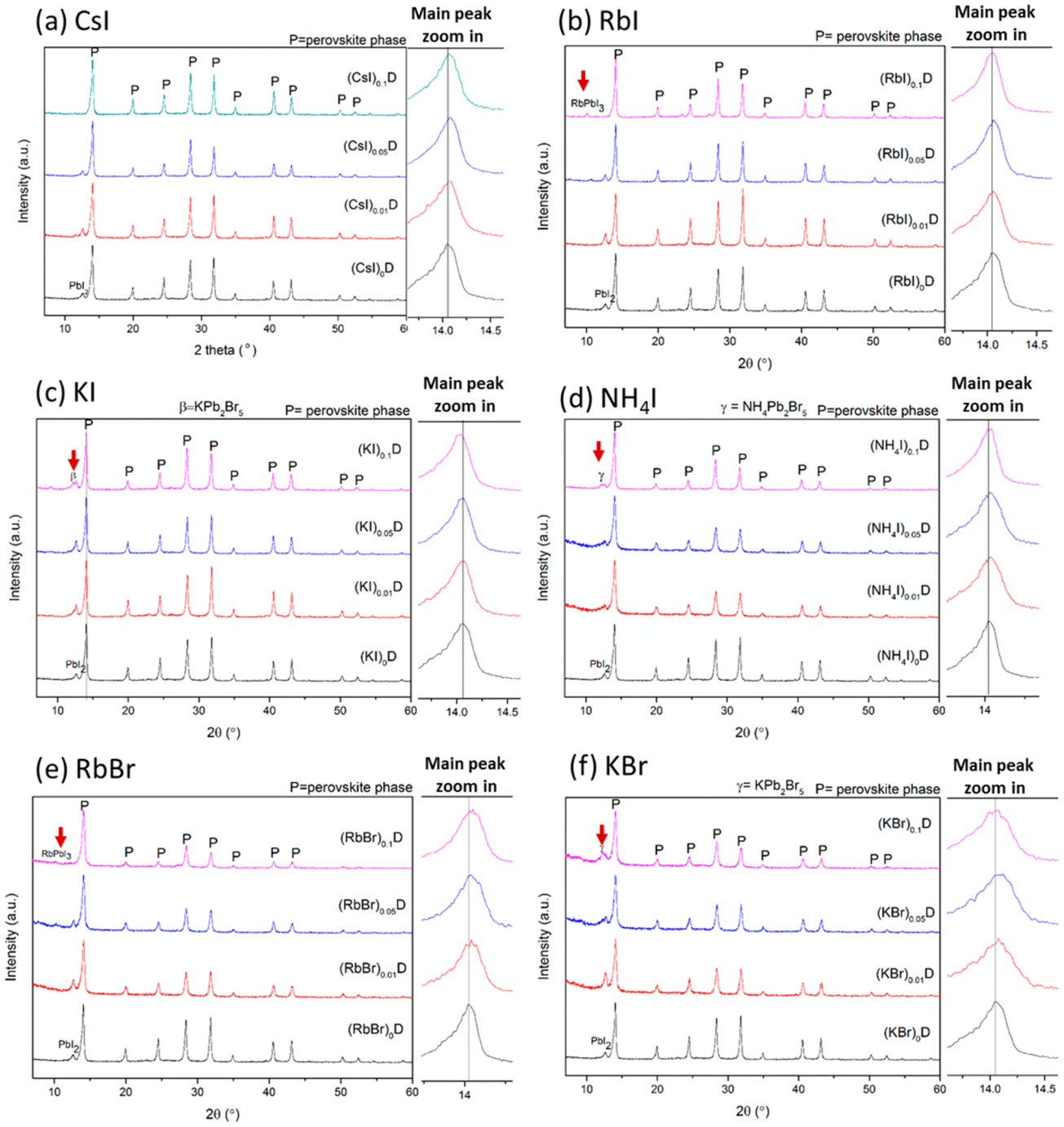

Figure 2. X-ray diffraction patterns of double cation perovskite films $[(MAPbBr_3)_{0.15}(FAPbI_3)_{0.85}]$ prepared using different additives (a) CsI, (b) RbI, (c) KI, (d) NH_4I, (e) RbBr, and (f) KBr, with different mole percentages. The red arrow marks the nonperovskite phase and magnifying patterns of main peak at around $2\theta = 14.07°$ are shown in the right side of the graph.

"forbidden zone", the overall system's τ is not a simple matter of rule of mixture calculation. Too much additives from the forbidden zone is bound to induce nonperovskite phases. Judging of this amount depends on the ionic size difference. The maximum "solubility" decreases as the difference in the ionic sizes gets big. In other words, only a very small amount can be added without inducing nonperovskite phase if small size cations are added into a bigger ionic size matrix.

Besides stabilizing the perovskite phase, we believe that the cations and anions inside the additives might affect the defect density of the matrix depending on their ionic sizes. As discussed afore, the dominant defects in perovskite are point defects, and it might be possible that the cation and anion satisfy the respective cation and halogen vacancies, or change the formation energy of defects. The cation/anion having small ionic size difference with that of matrix ions should be a better choice for defect passivation.

The additive approach have been demonstrated previously for phase stabilization, here in this work we will focus more on the defect passivation effect. To verify this, cations in "lower forbidden zone" (K, Rb, NH_4) and "cubic perovskite formation zone" (Cs) were experimentally verified. In order to investigate

DOI: 10.1021/acs.jpcc.8b00980
J. Phys. Chem. C 2018, 122, 13884−13893

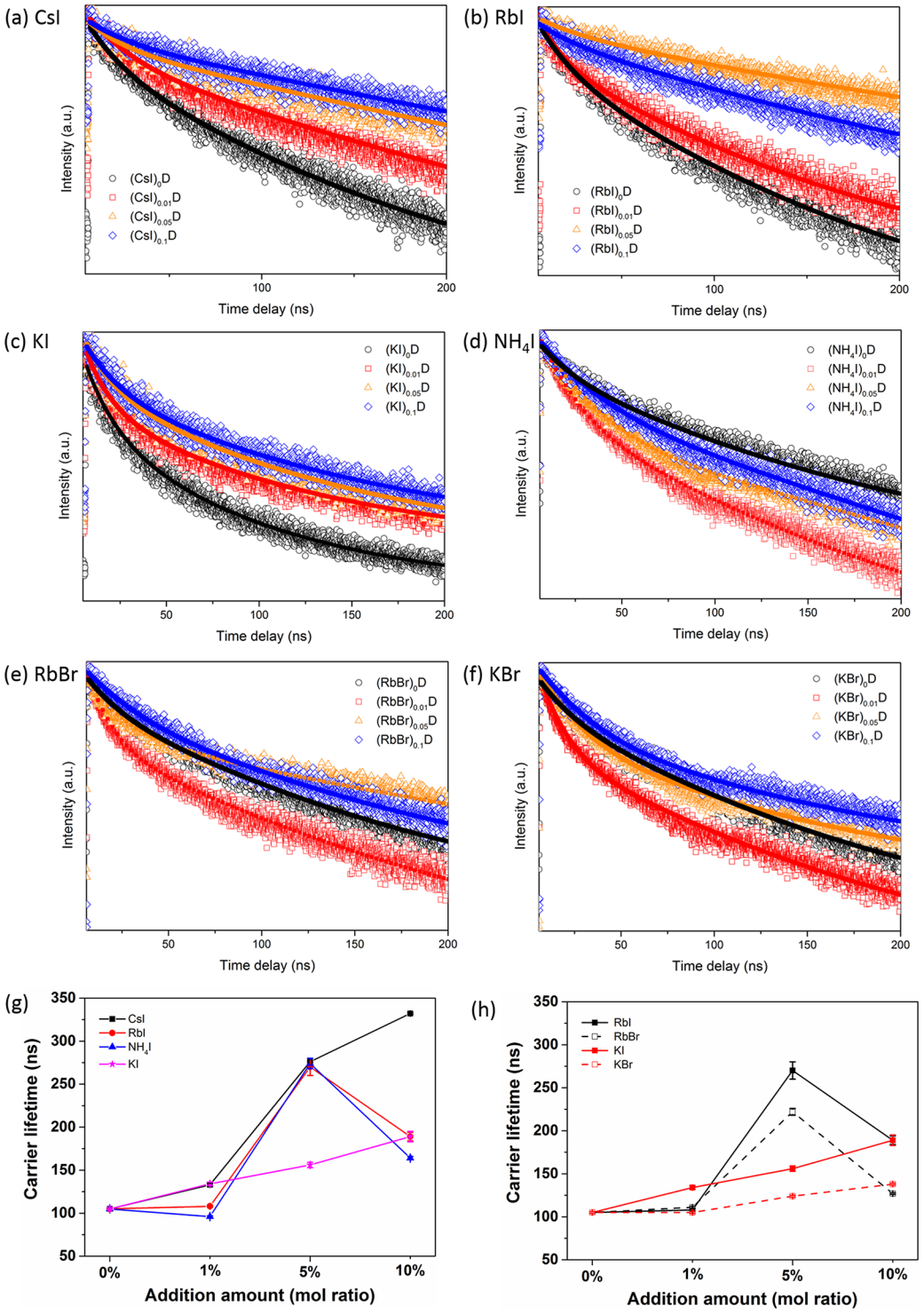

Figure 3. Time resolution photoluminescence (TRPL) analysis of perovskite films prepared using double cation perovskite $(MAPbBr_3)_{0.15}(FAPbI_3)_{0.85}$ with different cations as additives of (a) CsI, (b) RbI, (c) KI, (d) NH_4I, (e) RbBr, and (f) KBr Bi-exponential decay equations, $y = y_0 + A_1e^{-(x-x_0)/t_1} + A_2e^{-(x-x_0)/t_2}$, were used to fit the data. The variation of charge carrier lifetime of the perovskites films $(MAPbBr_3)_{0.15}(FAPbI_3)_{0.85}$ prepared using the (g) different cation (CsI, RbI, NH_4I, and KI) addition in various mole percentages. (h) Comparison in charge carrier lifetime measurements obtained from the perovskite film prepared using the KI, KBr, RbI and RbBr, i.e., different halides as additives (iodide and bromide salts).

the anion effect, both iodide and bromide salts of same cation were chosen (e.g., KI and KBr). We prepared perovskite films using double-cation mixed halide perovskite $[(MAPbBr_3)_{0.15}(FAPbI_3)_{0.85}]$ as matrix and added different amount of additives, i.e., KI, KBr, RbI, RbBr, NH_4I, and CsI. The perovskite matrix has a τ value of 0.98 (based on the mixing rule calculation), right within the stable perovskite phase formation range, i.e. $0.8 < \tau < 1$. With addition of 1%, 5%, and 10% of each salt, τ values of the system are in the range of 0.95 to 0.98 based on mixing rule. As indicated in Figure 1, the excess amount additives belonging to lower forbidden zone may introduce a secondary nonperovskite phase. To confirm this, the

DOI: 10.1021/acs.jpcc.8b00980
J. Phys. Chem. C 2018, 122, 13884−13893

X-ray diffraction (XRD) patterns of thus prepared perovskite films are presented in Figure 2. The perovskite films prepared without any additive exhibit a small peak at $2\theta = 12.5°$ assigned to PbI_2 and all other characteristic peaks attributed to black perovskite phase. Here, the perovskite precursor solution (matrix material) was prepared using the 10% mole excess of PbI_2 based on the earlier reported method, as excess PbI_2 could enhance the performance of double cation mixed halide perovskite solar cells.[38] As shown in Figure 2a, there was no obvious change in the XRD pattern of the perovskite films observed after CsI addition up to 5%. Surprisingly, the PbI_2 peak ($2\theta = 12.5°$) disappeared after 10% CsI addition, likely due to the reaction between CsI with PbI_2 to form $CsPbI_3$. Interestingly, at 10% CsI addition pure perovskite phase formation was observed and no significant shift in the characteristic peak position of perovskite $2\theta = 14.07°$ was observed (Figure 2a). In case of RbI addition, the recorded XRD patterns was invariant until 5% (Figure 2b), however, at 10%, the peak due to PbI_2 disappeared and the new peak at low angle ($2\theta = 11.07°$) appears, hinting at the formation of the nonperovskite phase of $RbPbI_3$. Similarly, for addition of KI, NH_4I, RbBr, and KBr, the maximum additive amount without producing nonperovskite phase was 5% (Figure 2c–f). At 10% addition, though there was no apparent peak shift in the characteristic peak position as compared to parent perovskite, but the nonperovskite phase formation was confirmed by low angle peaks ($2\theta = 11.07°$). Though the τ values of perovskite films with 10% addition of additives are right in the range of $0.8 < \tau < 1.0$ according to the mixing rule calculation, still the secondary nonperovskite phase formation was noted. Therefore, the amount of cation additives belonging to the "forbidden zone" needs be optimized experimentally to avoid the nonperovskite phase formation. From the above data, it has been summarized that all the additives experimented, i.e., KI, KBr, NH_4I, RbI, and RbBr, induce nonperovskite phase formation with 10% addition except CsI (belongs to cubic perovskite formation zone). This observation is consistent with our prediction based on tolerance factor analysis.

It is recommended that the additives should improve the performance of matrix perovskite without altering its bandgap and absorption edge. Accordingly to verify the above mention claim, the UV–visible measurements of the perovskite films with different additives have been carried out and corresponding Tauc plots have been calculated (Figure S1). Maximum of 0.02 eV blue shift in the bandgap value of the perovskite films was noted with addition of additives up to 10%, which is close to the measurement sensitivity limit of the instrument. The observed shift in the bandgap is almost negligible and indicates the desired amount in terms of additive selection (<10%).

Generally, the charge carrier lifetime of resultant perovskite films is longer than that of the matrix if the additive do passivate the defects inside the matrix. To verify this, the time-resolved photoluminescence (TRPL) measurements were conducted (Figure 3). All the decays follow a bi-exponential decay trend described by $y = y_0 + A_1 e^{-(x-x_0)/t1} + A_2 e^{-(x-x_0)/t2}$. The data have been fitted accordingly and the carrier lifetime extracted in Figure 3g,h and Table S2. Only the slow decay time is presented here as it is more related to the solar cell performance. With the addition of CsI, the average charge carrier lifetime of perovskites systematically increases from 105 ± 1 ns (0%) to 332 ± 1 ns (10%). However, with RbI and NH_4I addition, the carrier lifetime increases up to 5% addition (270 ± 10 ns and 274 ± 6 ns respectively) and then further increases in the addition amount up to 10%, with a shorter carrier lifetime (189 ± 5 ns and 164 ± 2 ns respectively) in Figure 3g and Table S2, which might relate to the nonperovskite phase formation. In case of KI additive, the carrier lifetime continuously climbs up from 105 ± 1 ns (0%) to 189 ± 6 ns for 10% addition. However, the obtained charge carrier lifetime at 10% KI addition is still shorter as compared to other additives. In brief, carrier lifetimes obtained for the perovskite films prepared with 5% RbI and NH_4I addition are 270 ± 10 ns and 274 ± 6 ns respectively, which are longer than that with 10% KI addition (189 ± 6 ns) (cf. Figure 3g and Table S2). As Cs is within the "cubic perovskite formation zone", therefore, it is not surprising that maximum lifetime (332 ± 1 ns) is achieved with 10% CsI addition, higher than that of films from all the other cations within the "forbidden zone", which is consistent with the XRD analysis. In summary, addition of additives involved in this work increases the carrier lifetimes of perovskite films, and the process is more efficient when the additive is from the cubic perovskite formation zone since the structural modification is less pronounced.

Usually charge carrier lifetime is strongly related to the defect/trap densities inside the semiconductor, especially nonradiation recombination. As mentioned previously, point defects such as vacancies (V_{MA}, V_{Pb} and V_I) and interstitials (MA_i, Pb_i and I_i) are dominant defects in perovskite.[3,26,27] All cations (K, Rb, NH_4, Cs) added as additives have smaller ionic sizes than those of MA and FA inside the matrix. These cations could be properly fill into the vacancies of MA and/or FA, or enter into the interstitial places of MA and/or FA to passivate defects. It might also be possible that the addition of these cations increase the formation energy of these point defects and thus decrease the defect density. These results necessitate theoretical calculation of defect formation energy with different additives to be fully understood, which is out of the scope of this current study. As the ionic size increases from K, NH_4, Rb to Cs, the Cs has smallest size difference with MA and FA than that of other additive cations. Therefore, the defects passivation effect is more promising with Cs than with any others, coinciding with the longest carrier lifetime of perovskite film with 10% CsI addition. NH_4 and Rb cations have similar ionic size, and their effects on the charge carrier lifetime are analogous. As the K is the smallest cation, it is logical that larger amount is need to have similar defect passivation effect with bigger cation. The defect passivation effect becomes more efficient as the difference in the ionic sizes gets smaller. Through theoretical calculation, Son et al.[24] suggest that the K cation mostly enters into the interstitial site preventing the formation of an iodine Frenkel defect. These results are in agreement with previous work in which we proved that using MABr to passivate the defects in the $Cs_{0.05}(MA_{0.15}FA_{0.85})_{0.95}Pb(Br_{0.15}I_{0.85})_3$ matrix decreases the trap density and increases the solar cell efficiency with 2% absolute value.[30]

To study the anion effect, the charge carrier lifetime measurements were performed using RbI and RbBr, KI and KBr as additives given in Figure 3h and Table S2. The solid line represents the measured carrier lifetime of perovskite films with iodide salt addition while the dash line stands for the bromide counterpart. The longer carrier lifetime was obtained for the perovskite films prepared using the iodide anion containing additives (e.g., RbI 270 ± 10 ns vs RbBr 222 ± 4 ns; KI 189 ± 6 ns vs KBr 138 ± 1 ns) as compared to that of bromide compounds. This strongly indicates that the types of anion inside an additive do affect the performance of perovskite films. Because of the higher formation energy of bromine vacancy,[39,40] iodine vacancy should be the dominant defect in the matrix perovskite. Therefore, the iodine anion (I) is more efficient in passivation

DOI: 10.1021/acs.jpcc.8b00980
J. Phys. Chem. C 2018, 122, 13884–13893

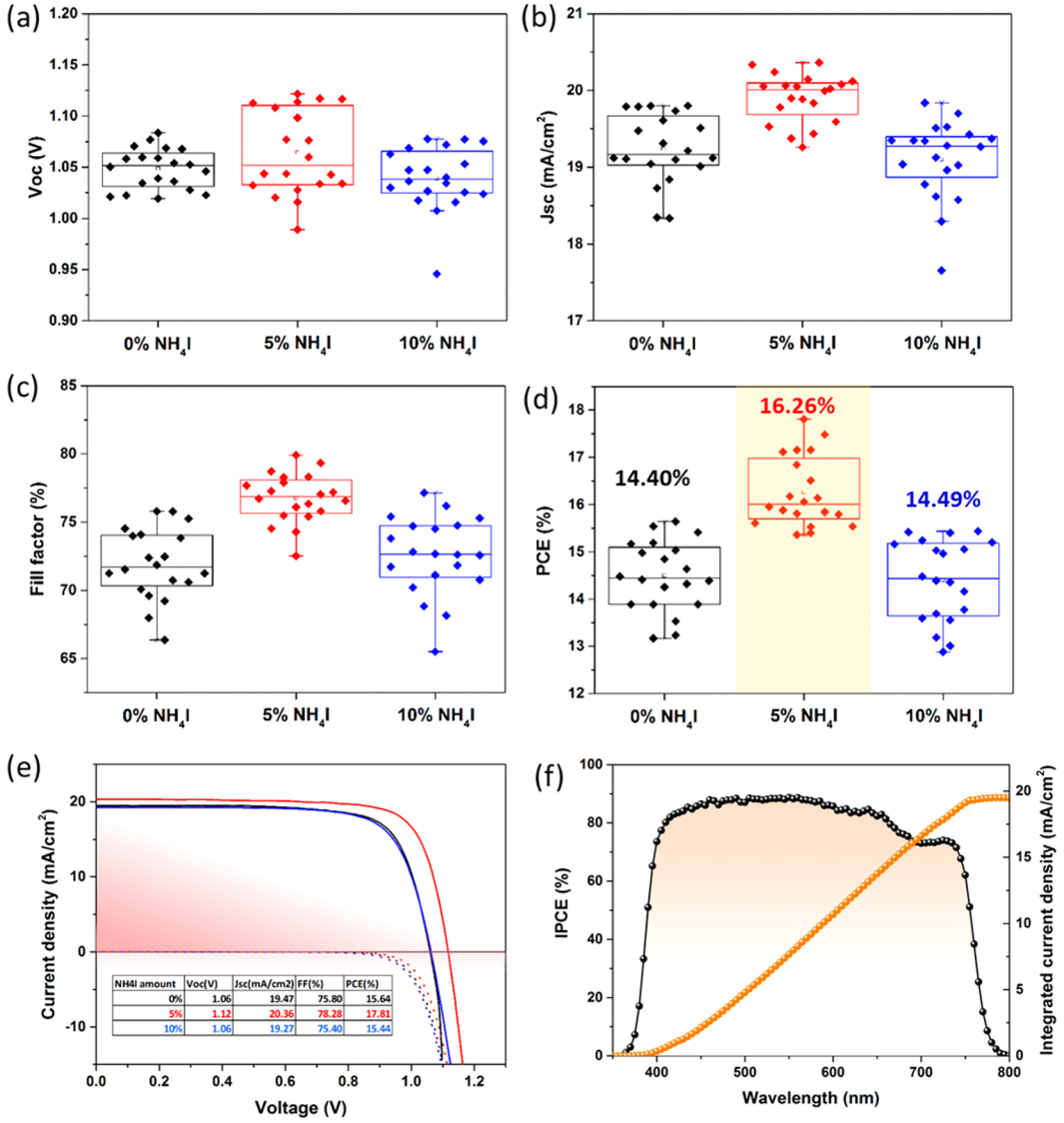

Figure 4. Device performance distribution of characteristic photovoltaic parameters obtained from perovskite based solar cell, perovskite film were fabricated using the addition of NH_4I as an additive in double cation perovskite $(MAPbBr_3)_{0.15}(FAPbI_3)_{0.85}$ at different mole % i.e. 5% and 10%: (a) open-circuit voltage (V_{oc}), (b) short-circuit current density (J_{sc}), (c) fill factor (FF), and (d) power conversion efficiency (PCE) at similar device fabrication conditions. The device distribution was collected over the 20 devices for each fabrication condition with NH_4I as an additive. The device performance was measurement under standard one sun illuminance condition. (e) Characteristic current density (J_{sc}) vs voltage (V) curves of the champion cell fabricated using the perovskite film prepared using double cation perovskite $(MAPbBr_3)_{0.15}(FAPbI_3)_{0.85}$ with NH_4I as an additive at different mole % i.e. 0%, 5% and 10% (mole percentage), inset shows the characteristic device parameters. (f) Incident photon-to-current efficiency (IPCE) of the best performing device. Solar cells with active area of 5×5 mm^2 are measured under one sun illumination condition with a 3×3 mm^2 metal mask to precisely confine the area. The efficiency was obtained from a reverse scan with a scan rate of 0.1 V/s.

of these iodine defects than smaller bromine anion (Br), confirming experimentally from the longer carrier lifetime with iodide additives. This clearly reveals that not only the cation but also the anion play important roles in terms of defect passivation and enhance the performance of perovskite based films. Seok et al.[41] have reported that 3% iodine addition during fabrication of perovskite enhances the device efficiency, which is attributed to compensation of iodine deficient and filling up of vacancies. The report well supports our results that anion additives do have big effect on the performance of perovskites. Overall, CsI addition exhibits the more pronounced trap/defect passivation effect as compared to other additives and iodine anion is preferred over the bromine one. In summary, to passivate the defects, small ionic size difference is preferred.

It was also reported that the charge carrier lifetime may differ with perovskite grain size.[42,43] In general, longer charge carrier lifetime is observed for perovskite films consisting of larger grain size i.e. less defects states. In order to validate this result, FESEM images of the perovskite films prepared with different additives were performed. We compared the morphology of perovskite films prepared with 10% additive addition, as the charge carrier lifetime values show a drastic variation with types of additives (Figure S2). With 10% addition of CsI, the grain size of perovskite film became smaller than that of the film without any additives. With 10% addition of RbI and KI, the grain size seems to be slightly increased. In case of the bromide salt addition, the bromide perovskite has lower melting point compared to iodide counterpart, therefore larger grain size formation is expected through Ostwald ripening. However, no significant grain size

DOI: 10.1021/acs.jpcc.8b00980
J. Phys. Chem. C 2018, 122, 13884−13893

difference is observed, which might be due to the poor solubility of bromide salt. Nevertheless, no clear trends have been observed in the grain size of perovskite films prepared using different types of additives. This is inconsistent with the charge carrier lifetime measurement where notable increment in the charge carrier lifetime of perovskite films with additive addition was observed. Therefore, the observed improvement in the carrier lifetime could not due to the grain size effect but attribute to the trap/defect passivation by additives. Cations inside these additives passivate the cation defects, while the anions fill the iodine vacancies, which might induce less trap states and thus longer carrier lifetime unless and until there is nonperovskite phase formation.

In selection of additives, two aspects of the ionic size should be considered simultaneously: (i) for purpose of passivating the point defects, small or even no size mismatch of cation/anion between additive and matrix is the best; (ii) for purpose of stabilizing the perovskite structure, larger mismatch benefits.

The effect of CsI and RbI addition on device performance of double cation perovskite has been reported by several groups as mentioned previously. The study clearly reveals that CsI and RbI addition up to 5% improved the device performance in comparison with the device fabricated without any addition.[15,18]

On the basis of optoelectronic study of perovskite films with different additives, full solar cell devices were prepared using NH_4I (Figure 4), and KI (Figure S3) as prototype additives with 0%, 5% and 10% addition. The device data collected over 20 devices for each condition in Figure 4. The average power conversion efficiency (PCE) of the perovskite solar cells was increased from 14.40% to 16.26% with 5% NH_4I addition, however, it decreases with 10% NH_4I (14.49%) addition. Around 2% absolute PCE improvement is noted with 5% NH_4I addition. The obtained PCE result is in good agreement with the carrier lifetime measurement, i.e. PCE and charge carrier lifetime improve with NH_4I addition and reach maximum at 5%. The characteristic current−voltage (J vs V) curve of champion cells fabricated using perovskite with 5% NH_4I addition is shown in Figure 4e. At 5% NH_4I addition, increments in V_{oc} (from 1.06 to 1.12 V), J_{sc} (from 19.47 mA/cm^2 to 20.36 mA/cm^2), fill factor (FF) (from 75.80% to 78.28%), and hence efficiency (PCE) (from 15.64% to 17.81%) were observed as compared to the control cell. The incident photon-to-current efficiency measurement supports the good performance of champion device as shown in Figure 4f. With addition of KI, the efficiency improves at 5% then drops at higher concentration (Figure S3), which is consistent with the XRD results. The improved performance with 5% NH_4I or KI addition supports the validity and reliability of our prediction. Our results are also in good agreement with the recently reported work based on the KI addition.[25] The relative improvement of average PCE is about 12.9% for 5% NH_4I addition. Other report also showed that at 7.5% KI addition into $CsPbI_2Br$, the efficiency increases from 8.2% to 9.1% with a relative improvement of 11%.[21] With 5% Cs addition into $(MA_{0.17}FA_{0.83})Pb(I_{0.83}Br_{0.17})_3$ forming triple-cation system, the average PCE increase from 16.37% to 19.2%.[15] Blending Rb into this triple-cation system further improves the PCE to 20.2%.[18] Thus, small amount of additive addition effectively improves the performance of perovskite solar cells mainly due to the defect passivation effect, indicating the importance and flexibility of composition design for perovskite systems.

The generality of the results presented can also be extended to the bromide perovskite system: $CsPbBr_3$, $FAPbBr_3$, and $MAPbBr_3$ are promising candidates for LED application. In order to enhance the LED device performance, efforts are still ongoing in the direction of adding different additives in the perovskite precursors to form compact films with small grains and reduce the defect density.[44−46] On the basis of $APbBr_3$ perovskites, calculated tolerance factors with different cations are plotted in Figure S4. We noticed a very similar observation, i.e., the commonly used cations, namely Cs^+, and MA^+, reveal the τ in the range $0.8 < \tau < 1.0$, indicating the "pure" perovskite phase formation alone with these cations, which can be used as additives to each other in unlimited amounta. While the group I alkali metal cation (Na, K, Rb) and NH_4 exhibit τ-values <0.8, cations FA, EA, and EDA each have a τ-value >1.0. All those cations cannot form the perovskite phase alone and hence restricted the addition to an optimum amount to modify the performance of perovskite matrix. For instance, the alkali metal cations (Na, K, Rb, and NH_4) may be suitable candidate additives to minimize the defect states without affecting other properties of the matrix. There should be a vast possibility and flexibility of composition design in perovskite systems for high performance photovoltaics and LED applications.

4. CONCLUSIONS

In summary, we have investigated the effect of different additives i.e. group I alkali metal cations (Na, K, Rb, NH_4, and Cs) and anions (Br and I) on the performance of double cation mixed halide $(MAPbBr_3)_{0.15}(FAPbI_3)_{0.85}$ perovskite films. On the basis of tolerance factor calculations, cations Cs, MA, and FA can form the perovskite phase alone and therefore can be used as additives without introducing any nonperovskite phases. While cations Na, K, Rb, NH_4, EA and EDA fall into the "forbidden zone" for perovskite formation as cations themselves, this is bound to induce a nonperovskite phase due to size constraint; hence, they can be used as additives at an optimum amount to modify the performance of matrix perovskite. In order to stabilize the perovskite phase, cations with larger ionic size differences between additive and matrix are preferred as long as there is no nonperovskite phase formation. XRD analysis confirmed that 10% addition of Na, K, Rb, and NH_4 is already too much resulting nonperovskite phase formation. Notable longer charge carrier lifetime of perovskite films obtained with all additives clearly indicates that not only cations but also anions in additives are playing a vital role in defect passivation of perovskite matrix. In terms of defect passivation, similar ionic size cation/anion with the matrix is better choice. We have also validated the effect of NH_4I as a prototype additive on the device performance. The PCE of devices prepared with 5% NH_4I addition shows 2% absolute value improvement as compared to that without addition, which coincides with the film study. This material design rule can extend to other fields such as LED and laser etc., where Na, K, Rb, and NH_4 compounds would be promising additives for $CsPbBr_3$. This work offers a pathway toward harnessing the multitude of perovskite compositions to achieve high performing solar cells and perhaps other optoelectronic devices. This work also necessitates theoretical investigation of defect physics with different additives in perovskite systems.

■ ASSOCIATED CONTENT

Supporting Information

The Supporting Information is available free of charge on the ACS Publications website at DOI: 10.1021/acs.jpcc.8b00980.

Tolerance factors calculation, Tauc plot, calculated charge carrier lifetime and surface morphologies of double cation

DOI: 10.1021/acs.jpcc.8b00980
J. Phys. Chem. C 2018, 122, 13884−13893

perovskite films with different additives, device efficiency with addition of KI, and calculated tolerance factors with different cations in $APbBr_3$ systems (PDF)

AUTHOR INFORMATION

Corresponding Authors

*(N.M.): E-mail: Nripan@ntu.edu.sg.
*(S. Z.): E-mail: samzhang@swu.edu.cn.
*(S.M.): E-mail: Subodh@ntu.edu.sg.

ORCID

Guifang Han: 0000-0001-6220-6424
Lydia Helena Wong: 0000-0001-9059-1745
Cesare Soci: 0000-0002-0149-9128
Nripan Mathews: 0000-0001-5234-0822
Subodh G. Mhaisalkar: 0000-0002-9895-2426

Notes

The authors declare no competing financial interest.

ACKNOWLEDGMENTS

The authors acknowledge funding from the National Research Foundation, Prime Minister's Office, Singapore, under its Competitive Research Program (CRP Award No. NRF-CRP14-2014-03) and through the Singapore–Berkeley Research Initiative for Sustainable Energy (SinBeRISE) CREATE Program; Nanyang Technological University start-up grants (M4080514 and M4081293); and the Ministry of Education Academic Research Fund Tier 1 grants (RG184/14, RG166/16 and RG101/15) and Tier 2 grants (MOE2016-T2-1-100, MOE2014-T2-1-044, MOE2015-T2-2-015, and MOE2016-T2-2-012).

REFERENCES

(1) Kojima, A.; Teshima, K.; Shirai, Y.; Miyasaka, T. Organometal Halide Perovskites as Visible-Light Sensitizers for Photovoltaic Cells. *J. Am. Chem. Soc.* **2009**, *131*, 6050–6051.

(2) De Wolf, S.; Holovsky, J.; Moon, S.-J.; Löper, P.; Niesen, B.; Ledinsky, M.; Haug, F.-J.; Yum, J.-H.; Ballif, C. Organometallic Halide Perovskites: Sharp Optical Absorption Edge and Its Relation to Photovoltaic Performance. *J. Phys. Chem. Lett.* **2014**, *5*, 1035–1039.

(3) Han, G.; Zhang, S.; Boix, P. P.; Wong, L. H.; Sun, L.; Lien, S.-Y. Towards High Efficiency Thin Film Solar Cells. *Prog. Mater. Sci.* **2017**, *87*, 246–291.

(4) Ono, L. K.; Raga, S. R.; Remeika, M.; Winchester, A. J.; Gabe, A.; Qi, Y. Pinhole-Free Hole Transport Layers Significantly Improve the Stability of $MAPbI_3$-Based Perovskite Solar Cells under Operating Conditions. *J. Mater. Chem. A* **2015**, *3*, 15451–15456.

(5) Zhou, Z.; Pang, S.; Ji, F.; Zhang, B.; Cui, G. Fabrication of Formamidinium Lead Iodide Perovskite Thin Films Via Organic Cation Exchange. *Chem. Commun.* **2016**, *52*, 3828–3831.

(6) Lee, J.-W.; Seol, D.-J.; Cho, A.-N.; Park, N.-G. High-Efficiency Perovskite Solar Cells Based on the Black Polymorph of $HC(NH_2)_2PbI_3$. *Adv. Mater.* **2014**, *26*, 4991–4998.

(7) Ye, T.; Jiang, X.; Wan, D.; Wang, X.; Xing, J.; Venkatesan, T.; Xiong, Q.; Ramakrishna, S. Ultrafast Photogenerated Hole Extraction/Transport Behavior in a $CH_3NH_3PbI_3$/Carbon Nanocomposite and Its Application in a Metal-Electrode-Free Solar Cell. *ChemPhysChem* **2016**, *17*, 4102–4109.

(8) Pellet, N.; Gao, P.; Gregori, G.; Yang, T. Y.; Nazeeruddin, M. K.; Maier, J.; Gratzel, M. Mixed-Organic-Cation Perovskite Photovoltaics for Enhanced Solar-Light Harvesting. *Angew. Chem., Int. Ed.* **2014**, *53*, 3151–3157.

(9) Binek, A.; Hanusch, F. C.; Docampo, P.; Bein, T. Stabilization of the Trigonal High-Temperature Phase of Formamidinium Lead Iodide. *J. Phys. Chem. Lett.* **2015**, *6*, 1249–1253.

(10) Jeon, N. J.; Noh, J. H.; Yang, W. S.; Kim, Y. C.; Ryu, S.; Seo, J.; Seok, S. I. Compositional Engineering of Perovskite Materials for High-Performance Solar Cells. *Nature* **2015**, *517*, 476–480.

(11) Jacobsson, T. J.; Correa-Baena, J. P.; Pazoki, M.; Saliba, M.; Schenk, K.; Grätzel, M.; Hagfeldt, A. Exploration of the Compositional Space for Mixed Lead Halogen Perovskites for High Efficiency Solar Cells. *Energy Environ. Sci.* **2016**, *9*, 1706–1724.

(12) Correa Baena, J. P.; Steier, L.; Tress, W.; Saliba, M.; Neutzner, S.; Matsui, T.; Giordano, F.; Jacobsson, T. J.; Kandada, A. R. S.; et al. Highly Efficient Planar Perovskite Solar Cells through Band Alignment Engineering. *Energy Environ. Sci.* **2015**, *8*, 2928–2934.

(13) Li, Z.; Yang, M.; Park, J.-S.; Wei, S.-H.; Berry, J. J.; Zhu, K. Stabilizing Perovskite Structures by Tuning Tolerance Factor: Formation of Formamidinium and Cesium Lead Iodide Solid-State Alloys. *Chem. Mater.* **2016**, *28*, 284–292.

(14) Lee, J.-W.; Kim, D.-H.; Kim, H.-S.; Seo, S.-W.; Cho, S. M.; Park, N.-G. Formamidinium and Cesium Hybridization for Photo- and Moisture-Stable Perovskite Solar Cell. *Adv. Energy Mater.* **2015**, *5*, 1501310.

(15) Saliba, M.; Matsui, T.; Seo, J.-Y.; Domanski, K.; Correa-Baena, J.-P.; Nazeeruddin, M. K.; Zakeeruddin, S. M.; Tress, W.; Abate, A.; et al. Cesium-Containing Triple Cation Perovskite Solar Cells: Improved Stability, Reproducibility and High Efficiency. *Energy Environ. Sci.* **2016**, *9*, 1989–1997.

(16) Service, R. F. Cesium Fortifies Next-Generation Solar Cells. *Science* **2016**, *351*, 113–114.

(17) Deepa, M.; Salado, M.; Calio, L.; Kazim, S.; Shivaprasad, S. M.; Ahmad, S. Cesium Power: Low Cs^+ Levels Impart Stability to Perovskite Solar Cells. *Phys. Chem. Chem. Phys.* **2017**, *19*, 4069–4077.

(18) Saliba, M.; Matsui, T.; Domanski, K.; Seo, J.-Y.; Ummadisingu, A.; Zakeeruddin, S. M.; Correa-Baena, J.-P.; Tress, W. R.; Abate, A.; Hagfeldt, A.; et al. Incorporation of Rubidium Cations into Perovskite Solar Cells Improves Photovoltaic Performance. *Science* **2016**, *354*, 206–209.

(19) Duong, T.; Wu, Y. L.; Shen, H.; Peng, J.; Fu, X.; Jacobs, D.; Wang, E.-C.; Kho, T. C.; Fong, K. C.; Stock, M.; et al. Rubidium Multication Perovskite with Optimized Bandgap for Perovskite-Silicon Tandem with over 26% Efficiency. *Adv. Energy Mater.* **2017**, *7*, 1700228.

(20) Yadav, P.; Dar, M. I.; Arora, N.; Alharbi, E. A.; Giordano, F.; Zakeeruddin, S. M.; Grätzel, M. The Role of Rubidium in Multiple-Cation-Based High-Efficiency Perovskite Solar Cells. *Adv. Mater.* **2017**, *29*, 1701077.

(21) Nam, J. K.; Chai, S. U.; Cha, W.; Choi, Y. J.; Kim, W.; Jung, M. S.; Kwon, J.; Kim, D.; Park, J. H. Potassium Incorporation for Enhanced Performance and Stability of Fully Inorganic Cesium Lead Halide Perovskite Solar Cells. *Nano Lett.* **2017**, *17*, 2028–2033.

(22) Tang, Z.; Bessho, T.; Awai, F.; Kinoshita, T.; Maitani, M. M.; Jono, R.; Murakami, T. N.; Wang, H.; Kubo, T.; et al. Hysteresis-Free Perovskite Solar Cells Made of Potassium-Doped Organometal Halide Perovskite. *Sci. Rep.* **2017**, *7*, 12183.

(23) Yang, Y.; Song, J.; Zhao, Y. L.; Zhu, L.; Gu, X. Q.; Gu, Y. Q.; Che, M.; Qiang, Y. H. Ammonium-Iodide-Salt Additives Induced Photovoltaic Performance Enhancement in One-Step Solution Process for Perovskite Solar Cells. *J. Alloys Compd.* **2016**, *684*, 84–90.

(24) Son, D.-Y.; Kim, S.-G.; Seo, J.-Y.; Lee, S.-H.; Shin, H.; Lee, D.; Park, N.-G. Universal Approach toward Hysteresis-Free Perovskite Solar Cell Via Defect Engineering. *J. Am. Chem. Soc.* **2018**, *140*, 1358–1364.

(25) Tang, Z.; Uchida, S.; Bessho, T.; Kinoshita, T.; Wang, H.; Awai, F.; Jono, R.; Maitani, M. M.; Nakazaki, J.; Kubo, T.; et al. Modulations of Various Alkali Metal Cations on Organometal Halide Perovskites and Their Influence on Photovoltaic Performance. *Nano Energy* **2018**, *45*, 184–192.

(26) Yin, W. J.; Shi, T.; Yan, Y. Unique Properties of Halide Perovskites as Possible Origins of the Superior Solar Cell Performance. *Adv. Mater.* **2014**, *26*, 4653–4658.

(27) Buin, A.; Pietsch, P.; Xu, J.; Voznyy, O.; Ip, A. H.; Comin, R.; Sargent, E. H. Materials Processing Routes to Trap-Free Halide Perovskites. *Nano Lett.* **2014**, *14*, 6281–6286.

DOI: 10.1021/acs.jpcc.8b00980
J. Phys. Chem. C 2018, 122, 13884–13893

(28) Wu, B.; Nguyen, H. T.; Ku, Z.; Han, G.; Giovanni, D.; Mathews, N.; Fan, H. J.; Sum, T. C. Discerning the Surface and Bulk Recombination Kinetics of Organic−Inorganic Halide Perovskite Single Crystals. *Adv. Energy Mater.* **2016**, *6*, 1600551.
(29) Zarazua, I.; Han, G.; Boix, P. P.; Mhaisalkar, S.; Fabregat-Santiago, F.; Mora-Seró, I.; Bisquert, J.; Garcia-Belmonte, G. Surface Recombination and Collection Efficiency in Perovskite Solar Cells from Impedance Analysis. *J. Phys. Chem. Lett.* **2016**, *7*, 5105−5113.
(30) Han, G.; Koh, T. M.; Lim, S. S.; Goh, T. W.; Guo, X.; Leow, S. W.; Begum, R.; Sum, T. C.; Mathews, N.; Mhaisalkar, S. Facile Method to Reduce Surface Defects and Trap Densities in Perovskite Photovoltaics. *ACS Appl. Mater. Interfaces* **2017**, *9*, 21292−21297.
(31) Giordano, F.; Abate, A.; Correa Baena, J. P.; Saliba, M.; Matsui, T.; Im, S. H.; Zakeeruddin, S. M.; Nazeeruddin, M. K.; Hagfeldt, A.; Graetzel, M. Enhanced Electronic Properties in Mesoporous TiO_2 Via Lithium Doping for High-Efficiency Perovskite Solar Cells. *Nat. Commun.* **2016**, *7*, 10379.
(32) Li, C.; Lu, X.; Ding, W.; Feng, L.; Gao, Y.; Guo, Z. Formability of ABX_3 (X = F, Cl, Br, I) Halide Perovskites. *Acta Crystallogr., Sect. B: Struct. Sci.* **2008**, *64*, 702−707.
(33) Goldschmidt, V. M. Crystal Structure and Chemical Combination. *Ber. Dtsch. Chem. Ges. B* **1927**, *60*, 1263−1296.
(34) Goldschmidt, V. M. Die Gesetze Der Krystallochemie. *Naturwissenschaften* **1926**, *14*, 477−485.
(35) Boix, P. P.; Agarwala, S.; Koh, T. M.; Mathews, N.; Mhaisalkar, S. G. Perovskite Solar Cells: Beyond Methylammonium Lead Iodide. *J. Phys. Chem. Lett.* **2015**, *6*, 898−907.
(36) Zhang, T.; Dar, M. I.; Li, G.; Xu, F.; Guo, N.; Grätzel, M.; Zhao, Y. Bication Lead Iodide 2D Perovskite Component to Stabilize Inorganic α-$CsPbI_3$ Perovskite Phase for High-Efficiency Solar Cells. *Sci. Adv.* **2017**, *3*, e1700841.
(37) Gholipour, S.; Ali, A. M.; Correa-Baena, J.-P.; Turren-Cruz, S.-H.; Tajabadi, F.; Tress, W.; Taghavinia, N.; Grätzel, M.; Abate, A.; Angelis, F. D.; et al. Globularity-Selected Large Molecules for a New Generation of Multication Perovskites. *Adv. Mater.* **2017**, *29*, 1702005.
(38) Bi, D.; Tress, W.; Dar, M. I.; Gao, P.; Luo, J.; Renevier, C.; Schenk, K.; Abate, A.; Giordano, F.; Correa Baena, J.-P.; et al. Efficient Luminescent Solar Cells Based on Tailored Mixed-Cation Perovskites. *Sci. Adv.* **2016**, *2*, e1501170.
(39) Luo, Y.; Khoram, P.; Brittman, S.; Zhu, Z.; Lai, B.; Ong, S. P.; Garnett, E. C.; Fenning, D. P. Direct Observation of Halide Migration and Its Effect on the Photoluminescence of Methylammonium Lead Bromide Perovskite Single Crystals. *Adv. Mater.* **2017**, *29*, 1703451.
(40) Azpiroz, J. M.; Mosconi, E.; Bisquert, J.; De Angelis, F. Defect Migration in Methylammonium Lead Iodide and Its Role in Perovskite Solar Cell Operation. *Energy Environ. Sci.* **2015**, *8*, 2118−2127.
(41) Yang, W. S.; Park, B.-W.; Jung, E. H.; Jeon, N. J.; Kim, Y. C.; Lee, D. U.; Shin, S. S.; Seo, J.; Kim, E. K.; Noh, J. H.; et al. Iodide Management in Formamidinium-Lead-Halide−Based Perovskite Layers for Efficient Solar Cells. *Science* **2017**, *356*, 1376−1379.
(42) Stranks, S. D.; Eperon, G. E.; Grancini, G.; Menelaou, C.; Alcocer, M. J. P.; Leijtens, T.; Herz, L. M.; Petrozza, A.; Snaith, H. J. Electron-Hole Diffusion Lengths Exceeding 1 Micrometer in an Organometal Trihalide Perovskite Absorber. *Science* **2013**, *342*, 341−344.
(43) Xiao, Z.; Dong, Q.; Bi, C.; Shao, Y.; Yuan, Y.; Huang, J. Solvent Annealing of Perovskite-Induced Crystal Growth for Photovoltaic-Device Efficiency Enhancement. *Adv. Mater.* **2014**, *26*, 6503−6509.
(44) Tan, Z.-K.; Moghaddam, R. S.; Lai, M. L.; Docampo, P.; Higler, R.; Deschler, F.; Price, M.; Sadhanala, A.; Pazos, L. M.; Credgington, D.; et al. Bright Light-Emitting Diodes Based on Organometal Halide Perovskite. *Nat. Nanotechnol.* **2014**, *9*, 687−692.
(45) Kulkarni, S. A.; Muduli, S.; Xing, G.; Yantara, N.; Li, M.; Chen, S.; Sum, T. C.; Mathews, N.; White, T. J.; Mhaisalkar, S. G. Modulating Excitonic Recombination Effects through One-Step Synthesis of Perovskite Nanoparticles for Light-Emitting Diodes. *ChemSusChem* **2017**, *10*, 3818−3824.
(46) Ng, Y. F.; Kulkarni, S. A.; Parida, S.; Jamaludin, N. F.; Yantara, N.; Bruno, A.; Soci, C.; Mhaisalkar, S.; Mathews, N. Highly Efficient Cs-Based Perovskite Light-Emitting Diodes Enabled by Energy Funnelling. *Chem. Commun.* **2017**, *53*, 12004−12007.

DOI: 10.1021/acs.jpcc.8b00980
J. Phys. Chem. C 2018, 122, 13884−13893